

SCIENTIFIC REPORTS

OPEN

Novel strategies to mimic transmembrane tumor necrosis factor-dependent activation of tumor necrosis factor receptor 2

Roman Fischer^{1,2}, Jessica Marsal¹, Cristiano Guttà¹, Stephan A. Eisler³, Nathalie Peters¹, John R. Bethea², Klaus Pfizenmaier¹ & Roland E. Kontermann¹

Tumor necrosis factor receptor 2 (TNFR2) is known to mediate immune suppression and tissue regeneration. Interestingly, the transmembrane form of tumor necrosis factor (tmTNF) is necessary to robustly activate TNFR2. To characterize the stoichiometry and composition of tmTNF during TNFR2 activation, we constructed differently oligomerized single chain TNF ligands (scTNF) comprised of three TNF homology domain (THD) protomers that mimic tmTNF. Using a variety of cellular and *in vivo* assays, we can show that higher oligomerization of the scTNF trimers results in more efficient TNF/TNFR2 clustering and subsequent signal transduction. Importantly, the three-dimensional orientation of the scTNF trimers impacts the bioactivity of the oligomerized scTNF ligands. Our data unravel the organization of tmTNF-mimetic scTNF ligands capable of robustly activating TNFR2 and introduce novel TNFR2 agonists that hold promise as therapeutics to treat a variety of diseases.

The tumor necrosis factor (TNF) superfamily is a family of different cytokines with various functions. Most ligands of the TNF family are synthesized as trimeric type II transmembrane proteins that can be released into a soluble form via proteolytic processing. The structural hallmark defining the TNF ligand family is the carboxy-terminal TNF homology domain (THD) which is composed of two stacked β -pleated sheets that adopt a conserved jellyroll-like tertiary fold¹⁻³. This structural composition leads to the self-association of TNF monomers into trimers and is necessary for receptor binding^{1,3}. Due to the carboxy-terminal localization of the THD, both the transmembrane form as well as soluble TNF ligands assemble into trimers. However, the THD-mediated receptor interaction alone is not necessarily sufficient to activate receptor-associated intracellular signaling pathways. For several members of the TNF receptor superfamily, the initial formation of ligand receptor complexes is followed by secondary multimerization into supramolecular clusters⁴⁻⁷.

Despite their similar trimeric organization, membrane-bound and soluble TNF ligands can differ in their activity. This difference is specifically obvious for the name-giving family member TNF. TNF is synthesized as a trimeric transmembrane protein (tmTNF; 26 kDa) that can be released into soluble circulating TNF homotrimers (sTNF; 51 kDa) via cleavage of the ectodomain by TNF α -converting enzyme (TACE/ADAM17)⁸. Trimeric sTNF tends to irreversibly dissociate at subnanomolar concentrations, thereby losing its bioactivity⁹. Dissociation and thus inactivation can be prevented by connecting three TNF monomers with short intramolecular peptide linkers, resulting in covalently stabilized single-chain TNF trimers (scTNF)¹⁰.

TNF can bind two structurally distinct transmembrane receptors, TNF receptor (TNFR) 1 and TNFR2, which have marked differences in expression patterns, structure, signaling mechanisms and functions¹¹⁻¹³.

Both tmTNF and sTNF can activate TNFR1 in the picomolar range, whereas TNFR2 is only robustly activated by tmTNF¹⁴. Different association/dissociation kinetics of the ligand/receptor complexes may contribute to the different TNFR activation capabilities of sTNF and tmTNF. Whereas sTNF has a remarkably high affinity for TNFR1 ($K_d = 1.9 \times 10^{-11}$ M), the affinity for TNFR2 is significantly lower ($K_d = 4.2 \times 10^{-10}$ M)¹⁵. The high affinity

¹Institute of Cell Biology and Immunology, University of Stuttgart, Allmandring 31, 70569, Stuttgart, Germany.

²Department of Biology, Drexel University, 3245 Chestnut Street, Philadelphia, PA, 19104, USA. ³Stuttgart Research Center Systems Biology, Nobelstraße 15, University of Stuttgart, Stuttgart, Germany. Correspondence and requests for materials should be addressed to R.F. (email: rf428@drexel.edu) or R.E.K. (email: roland.kontermann@izi.uni-stuttgart.de)

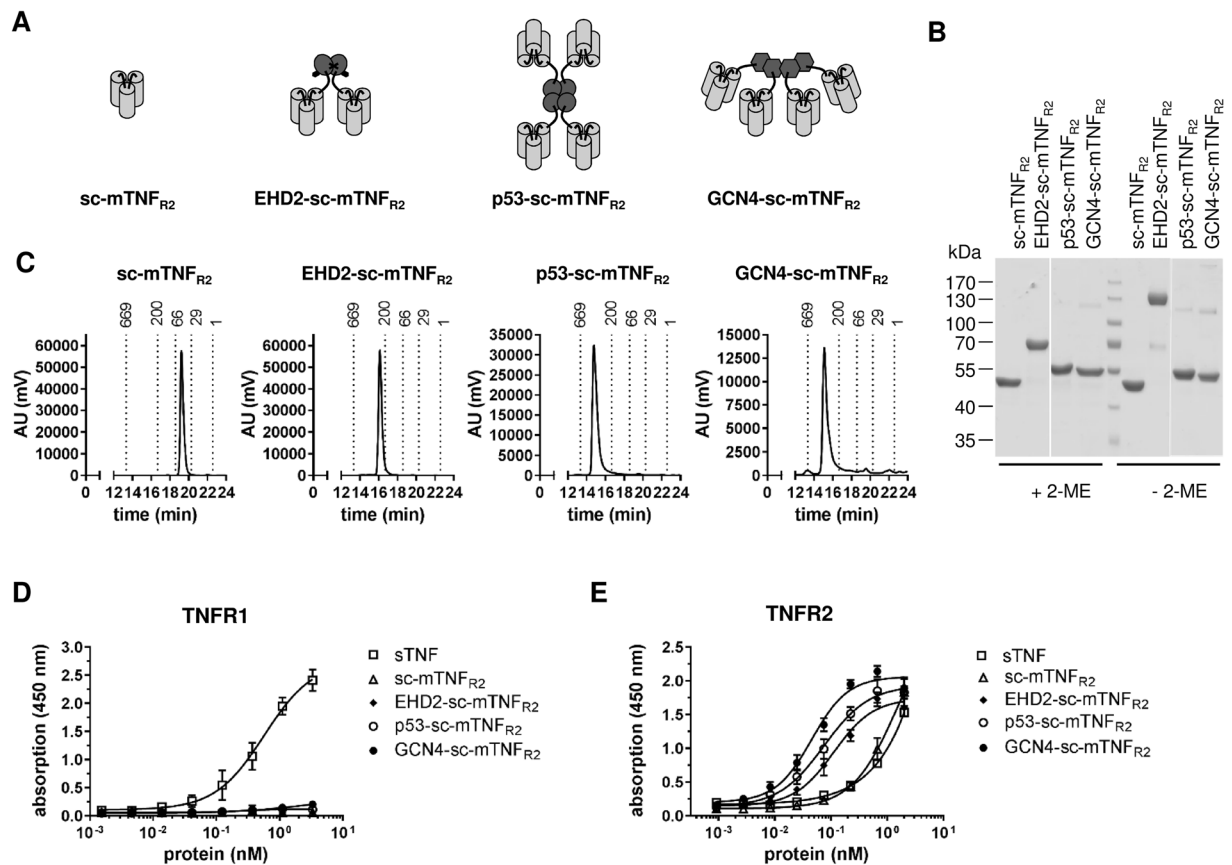


Figure 1. Characterization of oligomeric TNFR2 selective TNF muteins (A) Schematic representation and size exclusion chromatography analysis of the differently oligomerized TNF muteins sc-mTNF_{R2}, EHD2-sc-mTNF_{R2}, p53-sc-mTNF_{R2} and GCN4-sc-mTNF_{R2}. (B) Coomassie staining of sc-mTNF_{R2}, EHD2-sc-mTNF_{R2}, p53-sc-mTNF_{R2} and GCN4-sc-mTNF_{R2}. Purified TNF variants were analyzed by 8% SDS-PAGE under reducing (+2-ME) or non-reducing (-2-ME) conditions and stained with Coomassie. (C) Size exclusion chromatography analysis of the differently oligomerized TNF muteins sc-mTNF_{R2}, EHD2-sc-mTNF_{R2}, p53-sc-mTNF_{R2} and GCN4-sc-mTNF_{R2}. (D,E) Binding of the TNF muteins to mouse (D) TNFR1 and (E) TNFR2 was analyzed by ELISA. Soluble recombinant mouse TNF (sTNF) was used as a positive control for binding to TNFR1 (n = 3 ± SEM).

of sTNF for TNFR1 is mainly caused by stabilization of ligand/receptor complexes, while transient binding of sTNF to TNFR2 results in short-lived signal incompetent complexes^{15,16}.

A probable reason for the tmTNF-dependence for TNFR2 activation is the higher demand of TNFR2 for ligand-mediated crosslinking to allow signaling cluster formation^{16,17}. In this line, oligomerization of soluble ligand trimers, e.g. via antibody-mediated crosslinking, does not increase activation of TNFR1¹⁸, whereas secondary oligomerization of soluble TNF trimers converts this molecule into an active TNFR2 agonist^{19,20}.

To characterize the stoichiometry and composition of tmTNF necessary to efficiently activate TNFR2, we genetically engineered differently oligomerized TNFR2-selective scTNF ligands. The activity of these fusion proteins was then compared in regard to TNFR2 binding, TNF/TNFR2 complex formation and induction of specific cellular responses.

Results

Oligomerization of covalently stabilized scTNF dramatically improves affinity for TNFR2.

Previously, we demonstrated that oligomerized, covalently stabilized scTNF_{R2} mimics tmTNF and efficiently activates TNFR2^{19,21}. We, therefore, fused a mouse TNFR2-specific (D221N/A223R) sc-mTNF (sc-mTNF_{R2}) to different oligomerization domains, resulting in fusion proteins with different arrangements of the sc-mTNF_{R2} moieties (Fig. 1A, Fig. S1). For oligomerization, we applied the CH2 dimerization domain of IgE (EHD2^{21,22}), the tetramerization domain of p53 (aa 320–359)^{23–25} that exhibits an antiparallel arrangement of the domains (dimer of dimers) resulting in a tetrahedron-like 3D structure, and GCN4 (aa 249–281), a mutated helix from the yeast transcription factor GCN4^{24,26,27}, with a parallel arrangement of the four coiled-coil domains²⁸ (Fig. 1A). All fusion proteins were expressed in HEK293–6E cells, isolated by IMAC in a single step using a N-terminal his-tag present in the molecule and further purified by preparative size-exclusion chromatography (SEC). Purity was confirmed by SDS-PAGE and Coomassie staining (Fig. 1B). Under reducing conditions, the fusion proteins exhibited an apparent molecular mass of approximately 45 kDa (sc-mTNF_{R2}), 70 kDa (EHD2-sc-mTNF_{R2}) and

Protein	EC ₅₀ (nM)
sc-mTNF _{R2}	1.55
EHD2-sc-mTNF _{R2}	0.11
p53-sc-mTNF _{R2}	0.074
GCN4-sc-mTNF _{R2}	0.045

Table 1. Overview of the EC₅₀ values (nM) binding assay.

around 55 kDa (p53-sc-mTNF_{R2} and GCN4-sc-mTNF_{R2}), matching the calculated molecular mass of 50.2 kDa, 66.6 kDa, 59.7 kDa and 58.9 kDa for sc-mTNF_{R2}, EHD2-sc-mTNF_{R2}, p53-sc-mTNF_{R2} and GCN4-sc-mTNF_{R2}, respectively. Under non-reducing conditions, an additional band of approximately 140 kDa (dimer) was observed for EHD2-sc-mTNF_{R2}, indicating the disulfide-stabilized dimer formation via the EHD2 domain. Both p53-sc-mTNF_{R2} and GCN4-sc-mTNF_{R2} showed only partially oligomerized bands, which was expected since these oligomerization domains are not stabilized via covalent disulfide bonds. The oligomerization state of the fusion proteins was further confirmed by SEC (Fig. 1C). All fusion proteins eluted as a single major peak, indicating the integrity and high purity of the molecules. The apparent molecular masses correspond to the calculated molecular masses for monomers (50 kDa, sc-mTNF_{R2}), dimers (200 kDa, EHD2-sc-mTNF_{R2}) or tetramers (250 kDa, both p53-sc-mTNF_{R2} and GCN4-sc-mTNF_{R2}).

Binding of the fusion proteins to TNFRs was analyzed by ELISA using immobilized mouse TNFR1-Fc and TNFR2-Fc fusion proteins. No binding to TNFR1 was observed at any concentration tested (Fig. 1D), verifying that even highly oligomerized TNF muteins have lost their affinity towards TNFR1. In contrast, all scTNF_{R2} muteins bound to TNFR2. Whereas the monomeric sc-mTNF_{R2} (EC₅₀ value of 1.55 nM) only interacted with TNFR2 at high concentrations, similar to recombinant soluble TNF (sTNF), EC₅₀ values of EHD2-sc-mTNF_{R2} (EC₅₀ value of 0.11 nM), p53-sc-mTNF_{R2} (EC₅₀ value of 0.074 nM) and GCN4-sc-mTNF_{R2} (EC₅₀ value of 0.045 nM) were significantly lower, with GCN4-sc-mTNF_{R2} displaying the highest binding efficiency (Fig. 1E and Table 1).

Next, we used quartz crystal microbalance measurements to determine the affinity of the fusion proteins to mouse TNFR2-Fc. Using a high density chip (270 Hz) with saturated immobilized TNFR2, strong binding of sc-mTNF_{R2}, EHD2-sc-mTNF_{R2}, p53-sc-mTNF_{R2} and GCN4-sc-mTNF_{R2} to TNFR2 was observed, with K_d values between 61 to 44 pM (Fig. 2A and Table 2). In contrast, an around 10-times higher dissociation constants (K_d) was determined for sc-mTNF_{R2}. Minor differences were observed between EHD2-sc-mTNF_{R2}, p53-sc-mTNF_{R2} and GCN4-sc-mTNF_{R2}, with GCN4-sc-mTNF_{R2} showing the lowest off-rate. We, therefore, investigated, if differences between EHD2-sc-mTNF_{R2}, p53-sc-mTNF_{R2} and GCN4-sc-mTNF_{R2} can be detected using a low density chip (130 Hz), with non-saturated immobilized TNFR2 (Fig. 2B and Table 2). Interestingly, at lower receptor density the curves for p53-sc-mTNF_{R2} and GCN4-sc-mTNF_{R2} followed a biphasic binding to immobilized TNFR2. Indeed, for both p53-sc-mTNF_{R2} and GCN4-sc-mTNF_{R2} lower K_d values were measured compared to EHD2-sc-mTNF_{R2}, with GCN4-sc-mTNF_{R2} showing the most stable binding to the immobilized TNFR2.

TNFR2 selectivity of the oligomerized TNF muteins was confirmed using HeLa and L929 cells. In contrast to wild-type TNF used as a positive control, none of the TNFR2-selective fusion proteins induced TNFR1-dependent IL-6 secretion in HeLa cells (Fig. 3A). Furthermore, none of the fusion proteins activated TNFR1-dependent cell death in L929 (Fig. 3B), verifying that also the higher oligomerized p53-sc-mTNF_{R2} and GCN4-sc-mTNF_{R2} had lost affinity for TNFR1 and the capacity to activate this receptor.

Oligomerization of covalently stabilized scTNF is necessary for formation of higher order TNF/TNFR2 clusters.

Receptors of the TNF family are activated by ligand-mediated oligomerization²⁹ and efficient signal initiation requires the formation of larger ligand/receptor complexes^{16,30}. We, therefore, investigated the differences between the oligomeric TNF muteins to induce TNF/TNFR2 signaling cluster formation. Mouse BV-2 microglia cells were incubated with different concentrations of the fusion proteins and TNF/TNFR2 cluster formation was visualized via immune fluorescence (Fig. 4A,B). At low concentrations (0.1 nM), GCN4-sc-mTNF_{R2} induced the highest amount of TNF/TNFR2 signaling complexes, indicated by yellow spots due to colocalization of TNF (green) and TNFR2 (red) signals. Around 50% less TNF/TNFR2 signaling complexes were induced with p53-sc-mTNF_{R2}. Using a high concentration of 1 nM, similar efficient TNF/TNFR2 cluster formation (90–100%) was observed after incubation with p53-sc-mTNF_{R2} and GCN4-sc-mTNF_{R2}. In contrast, both scTNF_{R2} and EHD2-sc-mTNF_{R2} were less capable of inducing TNF/TNFR2 cluster formation, with 30–40% clusters formed at the highest concentration. Notably, at low concentrations (0.1 nM), almost no cluster formation was observed with sc-mTNF_{R2}, whereas EHD2-sc-mTNF_{R2} induced approximately 20% cluster formation.

Oligomerization of covalently stabilized scTNF is necessary to robustly mimic tmTNF.

We then investigated if the elevated binding capacity of the dodecavalent TNF oligomers is also converted to an increased bioactivity. First, we determined TNF_{R2}-induced secretion of Cxcl-2 in BV-2 cells. Here, GCN4-sc-mTNF_{R2} (EC₅₀ value of 32 pM) was 5-times more potent than p53-sc-mTNF_{R2} (EC₅₀ value of 130 pM) (Fig. 5A and Table 3). Furthermore, an approximately 3.5-times elevated bioactivity of p53-sc-mTNF_{R2} compared to EHD2-sc-mTNF_{R2} (EC₅₀ value of 438 pM) was observed, whereas sc-mTNF_{R2} induced the weakest Cxcl-2 secretion.

Bioactivity of the fusions proteins was further tested using Kym-1 cells that are highly sensitive for TNFR2-induced cell death³¹. Therefore, cells were incubated with the fusion proteins for 24 hours and cell

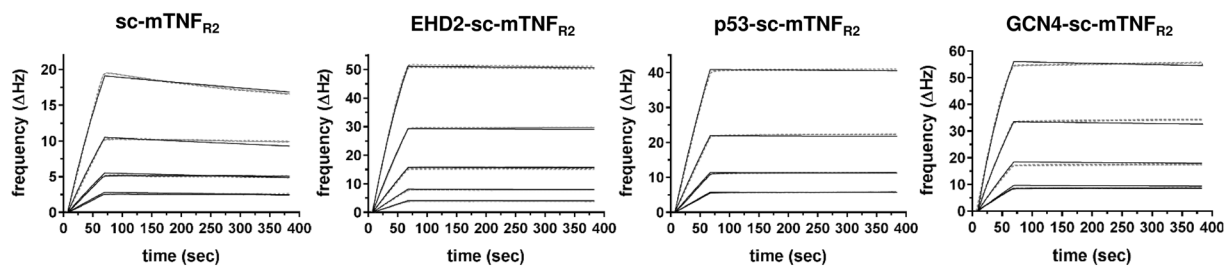
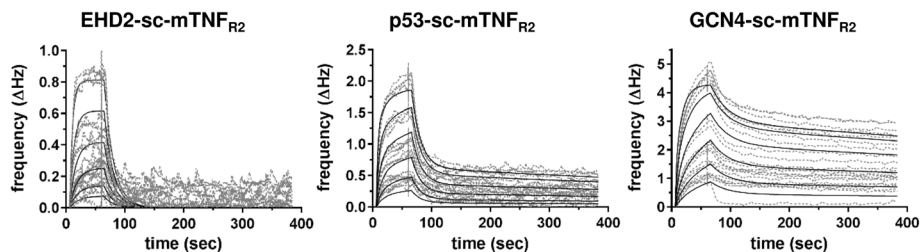
A High density chip (270 Hz)**B Low density chip (130 Hz)**

Figure 2. Dodecameric TNF muteins have higher affinity to TNFR2. Binding of oligomerized TNF muteins to mouse TNFR2 was analyzed by QCM at high (A; 270 Hz) and low (B; 130 Hz) density of immobilized mouse TNFR2-Fc. Oligomerized TNF muteins were analyzed at concentrations between 2–32 nM (A) or 8–256 nM (B) at 37 °C in triplicates for each concentration (dashed lines = data curves, solid lines = fitted curves).

	Protein	EHD2-sc-mTNFR ₂	p53-sc-mTNFR ₂	GCN4-sc-mTNFR ₂	sc-mTNFR ₂
high density	K_{on} ($M^{-1}s^{-1}$)	6.07×10^5	6.16×10^5	1.67×10^6	8.08×10^5
	K_{off} (s^{-1})	3.74×10^{-5}	2.69×10^{-5}	8.77×10^{-5}	3.99×10^{-4}
	K_d (nM)	0.0615	0.0437	0.0527	0.4494
low density	k_{on1} [$M^{-1}s^{-1}$]	5.33×10^5	1.28×10^6	2.16×10^6	n/d
	K_{off1} [s^{-1}]	6.3×10^{-2}	6.51×10^{-2}	3.47×10^{-2}	n/d
	K_{d1} (nM)	118	50.9	16.1	n/d
	k_{on2} [$M^{-1}s^{-1}$]	n/d	2.20×10^6	3.45×10^6	n/d
	K_{off2} [s^{-1}]	n/d	8.76×10^{-6}	5.97×10^{-6}	n/d
	K_{d2} (nM)	n/d	3.97	1.73	n/d

Table 2. QCM affinity measurements of oligomeric TNF muteins.

viability was measured using the crystal violet assay. Again, bioactivity was increased with higher oligomerization of the TNF muteins (Fig. 5B and Table 3). No significant TNFR2 signal induction was observed in this cellular system for sc-mTNFR₂ at the used concentrations. In contrast, p53-sc-mTNFR₂ induced an approximately 10-times stronger signal than EHD2-sc-mTNFR₂, whereas GCN4-sc-mTNFR₂ was 10-times more potent than p53-sc-mTNFR₂.

Next, we investigated TNFR2-induced proliferation of mouse thymocytes. Therefore, cells were incubated in presence of the different fusion proteins for 4 days and proliferation was determined by measuring their metabolic activity. All oligomerized fusion proteins induced proliferation. Whereas sc-mTNFR₂ only promoted proliferation at higher concentrations, all oligomerized fusion proteins efficiently induced proliferation (Fig. 5C and Table 3). Whereas p53-sc-mTNFR₂ (EC_{50} value 40 pM) was just slightly more potent than EHD2-sc-mTNFR₂ (EC_{50} value 55 pM), GCN4-sc-mTNFR₂ induced a more than 3-times increased response (EC_{50} value 16 pM) compared to EHD2-sc-mTNFR₂.

We next investigated TNFR2 signal induction in different immune cells (activated human and mouse T cells, regulatory T cells), known to express TNFR2^{32–34}. We choose to use a concentration of 0.3 nM of the fusion proteins, due to the different effects observed in the previous assays for this concentration. Similar results were obtained for both, TNFR2-induced expansion of human CD25⁺HLA-DR⁺ (Fig. 6A and Table S1) and mouse CD25⁺TNFR2⁺ (Fig. 6B) activated T cells. Thus, GCN4-sc-mTNFR₂ proved to be the strongest inducer of T cell proliferation, whereas no significant activity was recorded for sc-mTNFR₂ compared to control cultures. For both, human and mouse T cells, p53-sc-mTNFR₂ showed an apparent stronger activity than EHD2-sc-mTNFR₂, although the difference was statistically not significant. Since TNFR2 is a key marker of regulatory T cells

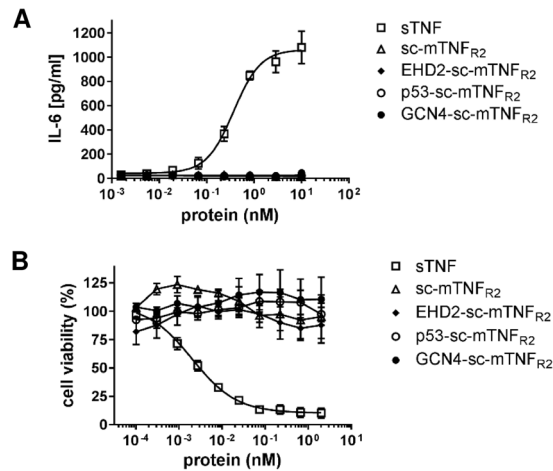


Figure 3. Dodecameric TNF muteins are still selective for TNFR2 (A) HeLa cells were stimulated with oligomerized TNF muteins for 24 hours. Soluble recombinant human TNF (sTNF) was used as a positive control for activation of TNFR1. Then supernatant was collected and analyzed for presence of IL-6 by ELISA ($n = 3 \pm \text{SEM}$). (B) L929 cells were incubated with oligomerized TNF muteins for 24 hours. Soluble recombinant mouse TNF (sTNF) was used as a positive control for activation of TNFR1. Cell viability was measured using crystal violet staining ($n = 3 \pm \text{SEM}$).

(Tregs)^{32, 34} and TNF is known to expand and stabilize Tregs via TNFR2^{32, 35–37}, we then investigated the potential of the different sc-mTNF_{R2} fusion proteins to expand Tregs. Therefore, CD3⁺ mouse T cells were activated using αCD3 , cultivated in presence of the tmTNF mimetics and the number of CD4⁺CD25⁺FoxP3⁺ Tregs was quantified by flow cytometry (Fig. 6C). Similarly to the previous experiments, the tetrameric GCN4-sc-mTNF_{R2} molecule was the most potent activator, inducing the strongest expansion of Tregs.

Dodecaivalent covalently stabilized scTNF show improved bioactivity *in vivo*. Recently, it was shown that *in vivo* application of a TNFR2 agonist leads to the expansion of Tregs and protects mice from acute graft versus host disease³⁸. Therefore, we administered low concentrations (1 mg/kg) of the TNF muteins EHD2-sc-mTNF_{R2}, p53-sc-mTNF_{R2} and GCN4-sc-mTNF_{R2} in mice and determined the number of CD4⁺CD25⁺FoxP3⁺ Tregs in the spleen after three days (Fig. 7A). Interestingly no significant activity of EHD2-sc-mTNF_{R2} compared with saline control was observed. In contrast, both p53-sc-mTNF_{R2} and GCN4-sc-mTNF_{R2} efficiently expanded Tregs at the applied dose of 1 mg/kg *in vivo*. No significant difference was observed between p53-sc-mTNF_{R2} and GCN4-sc-mTNF_{R2} at this dose. However, at a tenfold higher concentration (10 mg/kg) EHD2-sc-mTNF_{R2} induced an efficient expansion of Tregs, too (Fig. S2). The systemic tolerance of the oligomeric TNF fusion proteins was assessed by measuring the levels of C-reactive protein (CRP), a key inflammatory marker, in the blood (Fig. 7B). Neither 24 nor 72 hours after administration of the TNF muteins, altered CRP levels compared to saline-treated animals were observed.

Discussion

Several receptors of the TNF receptor superfamily depend on a transmembrane ligand to become robustly activated. Examples are the ligand/receptor pairs of CD95L and CD95, APRIL and TACI, OX40L and OX40, TRAIL and TRAILR2, and TNF and TNFR2^{14, 18, 39–41}. For mouse CD95L and TRAIL, soluble trimeric ligands solely containing the THD failed to bind to their cognate receptors and consequently were not able to activate receptor signaling. However, binding of these ligand variants to CD95 and TRAILR2 was restored by stabilization of the trimers via fusion to a trimerization domain. Although trimer stabilization restored receptor binding, this ligand still was not capable to efficiently activate its receptor⁴. Similar, covalent stabilization of TNF trimers improved the affinity to TNFR2, but did not improve the bioactivity¹⁰.

Previously, different approaches have been exploited to generate soluble TNF ligands mimicking the activity of the transmembrane form, e.g. by artificially increasing the avidity of TNF ligands through mutagenesis or by immobilizing them on a cell surface or the extracellular matrix (ECM). Antibody-mediated multimerization of Flag-tag-containing variants of soluble TNF, CD95L, TRAIL, and CD40L with Flag-specific antibodies resulted in a dramatic increase in avidity and efficient activation of their cognate receptors TNFR2, CD95, TRAILR2, and CD40, respectively^{30, 42, 43}. Similar, antibody-mediated cross-linking of TNFR2 via the monoclonal non-activating antibody 80M2 leads to pre-activation of TNFR2 on the cell surface, thereby mimicking receptor activation by the membrane form of TNF, if soluble recombinant TNF is added¹⁴. Genetic fusion of soluble CD95L, OX40L trimers to an oligomerization domain resulted in a dramatic increase in avidity and efficiently activated CD95 and OX40^{18, 30, 40}. Alternatively, immobilization of soluble ligands can elevate their activity. For instance, binding of soluble CD95L or soluble APRIL to components of the extracellular matrix converts these ligands into highly active cytokines^{44–46}. Similar data show that the activity of soluble trimeric variants of CD27L, CD40L, and 41BBL can be strongly increased by oligomerization or cell surface immobilization⁷.

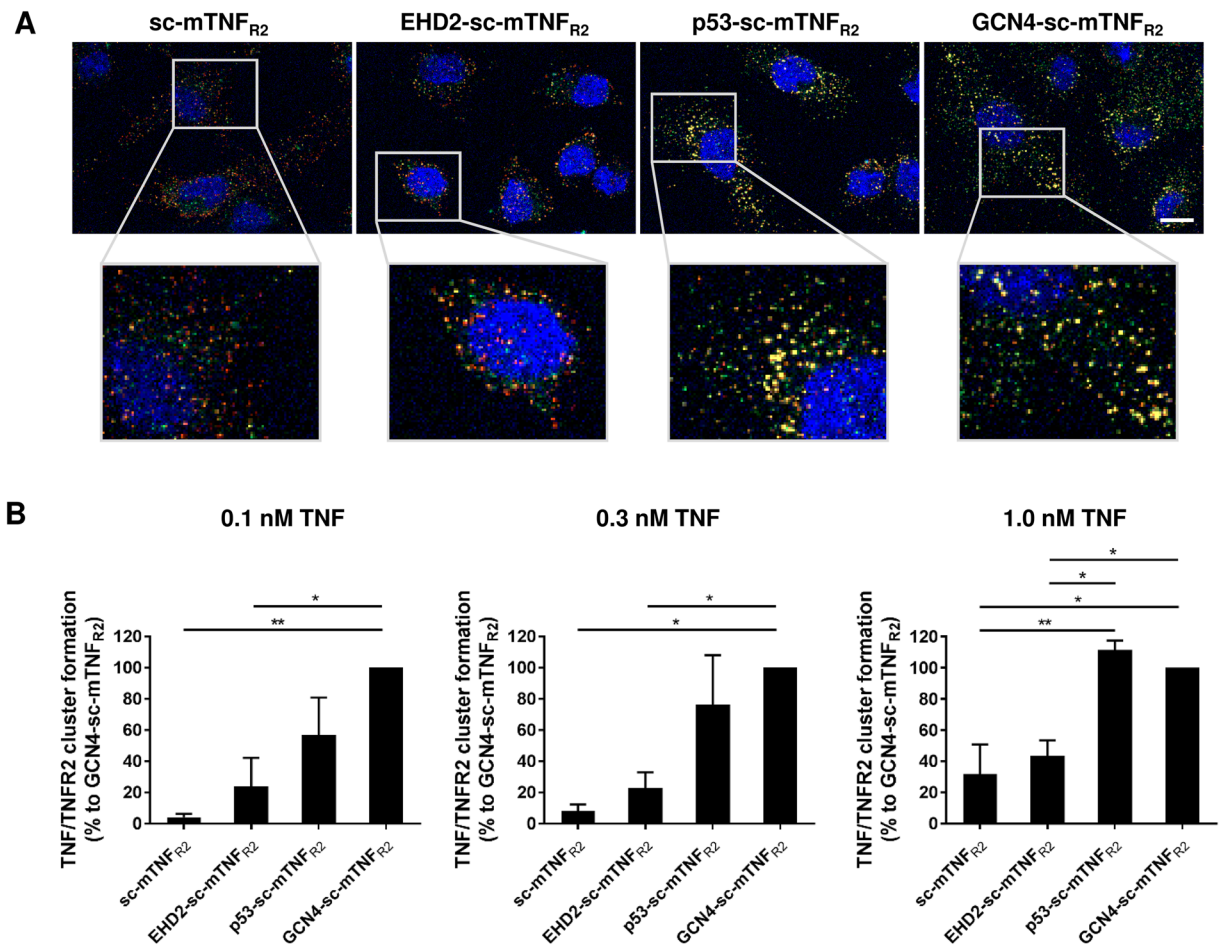


Figure 4. Dodecameric TNF mutants exert elevated TNF/TNFR2 cluster formation (A) BV-2 cells were incubated with the oligomerized TNF mutants (0.1, 0.3, 1.0 nM) for 15 minutes. Then cells were fixed and localization of TNFR2 (red) and oligomerized TNF mutants (green) was visualized by immunofluorescence microscopy. DAPI was used to counterstain cell nuclei. Fluorescence was analyzed using a Zeiss Axio Observer Spinning Disc microscope. Representative pictures for stimulation with 1 nM of the oligomerized TNF mutants are shown. Scale bar: 10 μ m. (B) Quantification of TNF/TNFR2 clustering ($n = 3 \pm$ SEM).

The dependence of the naturally occurring transmembrane ligand or membrane-mimetic variants for robust activation is especially obvious for TNFR2. Whereas it was shown that trimer stabilization both improves activation of TNFR1¹⁰ and TNFR2⁴⁷, oligomerization of trimeric TNF ligands is highly superior in activating TNFR2^{19–21}. In line with this, additional data indicate that mere mechanical fixation of TNF to an immobilized surface is insufficient to efficiently activate TNFR2. Rather, a certain density of the ligand and an additional stabilization of TNFR2 by cluster formation seems to be mandatory for efficient activation⁴⁸. Whereas data exist that oligomerization of a trimeric scTNF ligand improves its bioactivity, no data were available on the possible stoichiometry and composition of oligomerized TNF ligands necessary to robustly activate TNFR2.

Receptor binding studies revealed that the dodecavalent variants p53-sc-mTNFR₂ and GCN4-sc-mTNFR₂ both bind more stable to TNFR2 compared to the hexavalent EHD2-sc-mTNFR₂. Furthermore, using different cellular response assays, GCN4-sc-mTNFR₂ consistently exerted the highest bioactivity. In addition, in all assays a slightly increased bioactivity of p53-sc-mTNFR₂ compared to EHD2-sc-mTNFR₂ was observed. A first important step for efficient signal induction is the formation of higher order TNF/TNFR2 signaling clusters. Our microscopical analyses showed that GCN4-sc-mTNFR₂ efficiently promoted the cluster formation even at low sub-nanomolar concentrations. Likewise, p53-sc-mTNFR₂ was superior in cluster-formation compared to EHD2-sc-mTNFR₂, which translated into a 3.5-fold higher bioactivity in a Cxcl-2 chemokine secretion assay with BV-2 cells.

Altogether, our data show that the three-dimensional orientation of tmTNF-mimetic TNF ligands is important and determines the efficiency of TNFR2 signal induction. Our data suggest that the configuration of GCN4-sc-mTNFR₂ shares the highest similarity with the assumed natural tmTNF configuration, since all TNF trimers in the oligomer are arranged in a way that they point into the same direction. In contrast, p53-sc-mTNFR₂ seems to have more a spider-like shape in which the binding sites point into the directions of a tetrahedron²⁴. We, therefore, hypothesize that these different 3D-structures mainly impact the distance between the scTNF units, with the highly potent GCN4-sc-mTNFR₂ configuration displaying the least distance between the scTNF units.

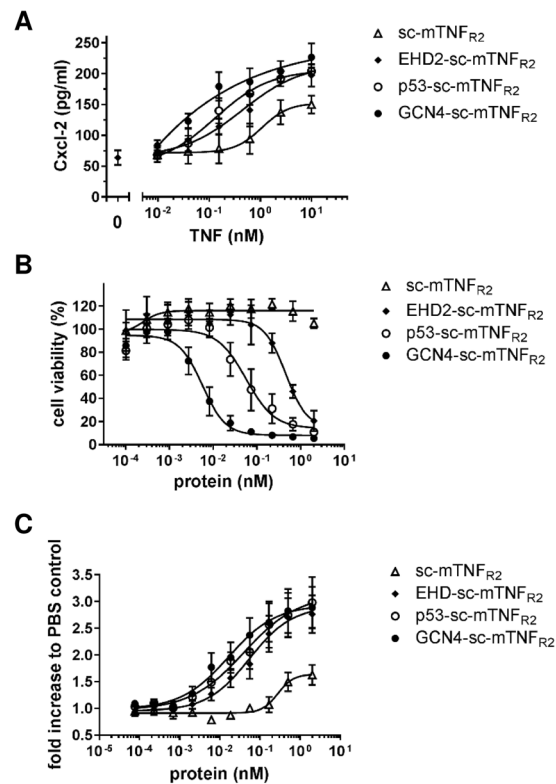


Figure 5. Dodecameric TNF mutants exert elevated bioactivity (A) BV-2 cells were incubated for 24 hours with the oligomerized TNF mutants. Then supernatant was harvested and analyzed for presence of secreted Cxcl-2 by ELISA ($n = 3 \pm \text{SEM}$). (B) Thymocytes were incubated for 4 days in presence of the oligomerized TNF mutants. Then metabolic activity was quantified to determine relative cell numbers ($n = 5 \pm \text{SEM}$). (C) Kym-1 cells were incubated for 24 hours with the oligomerized TNF mutants. Then cell viability was determined by crystal violet assay ($n = 4 \pm \text{SEM}$).

Protein	Cxcl-2 secretion (BV-2)	Cell death (Kym-1)	Proliferation (thymocytes)
sc-mTNF _{R2}	1071	n/d	277
EHD2-sc-mTNF _{R2}	438	453	55
p53-sc-mTNF _{R2}	130	56	40
GCN4-sc-mTNF _{R2}	44	5.7	16

Table 3. Overview of the EC₅₀ values (pM) bioactivity assays.

Therefore, it is likely that the distance between TNF trimers in tmTNF or tmTNF mimetic ligands also plays a role for the bioactivity. Interestingly, the *in vivo* application of the tetramers p53-sc-mTNF_{R2} and GCN4-sc-mTNF_{R2} is highly superior to dimeric EHD2-sc-mTNF_{R2}, whereas no significant differences between p53-sc-mTNF_{R2} and GCN4-sc-mTNF_{R2} were observed. This superior bioactivity of p53-sc-mTNF_{R2} *in vivo* compared to the *in vitro* assays might be due to possible *cis* and *trans* activation of TNFR2 on the same and on neighboring cells, respectively. We propose that a p53-sc-mTNF_{R2} molecule that binds to TNFR2s with a minimum of two scTNFs is capable of activating TNFR2, similar to EHD2-sc-mTNF_{R2}, but still possesses two free scTNFs capable of activating TNFR2 *in trans* on other cells. Keeping in mind that TNF/TNFR2 clusters are formed, such a higher order p53-sc-mTNF_{R2}/TNFR2 cluster with free scTNF molecules could mimic natural tmTNF signaling, i.e. an additional transactivation of a juxtaposed cell.

Since TNFR2 plays an important role in immune regulation and tissue regeneration, ligands that effectively activate TNFR2 hold great promise as novel therapeutics to treat a variety of diseases, including inflammatory and neurodegenerative diseases^{11, 13, 49, 50}. Drug potency and efficacy is of particular interest for therapeutic applications, as lower doses of the particular drug are needed to induce maximal therapeutic effects. Therefore the high and specific bioactivity of tmTNF-mimetic tetrameric scTNF oligomers represent a novel approach towards TNFR2-selective drugs.

In conclusion, we show that controlled oligomerization of scTNFs is a prerequisite to efficiently activate TNFR2. By introducing various oligomerization domains to generate dimeric or tetrameric scTNF ligands with different three-dimensional orientation of the scTNF units, we identified formats suitable for efficient TNF/

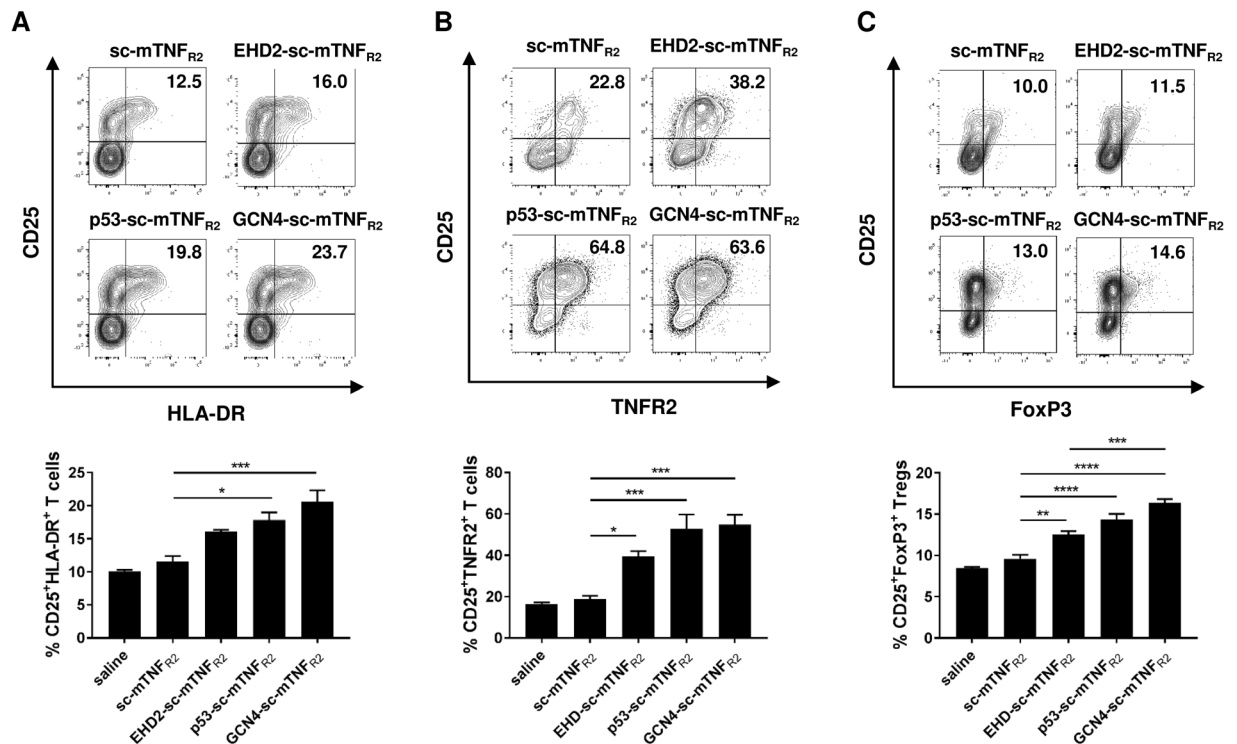


Figure 6. Dodecameric TNF mutants most potently induce T cell activation and Treg expansion (A) CD3⁺ T cells were isolated from human peripheral blood mononuclear cells (PBMCs) via magnetic separation. T cells were activated using plate-bound anti-CD3 (1 µg/ml) and cultivated in presence of interleukin 2 (IL-2, 10 U/ml) and 0.3 nM of the oligomerized TNF mutants for 4 days. Number of activated CD25⁺HLA-DR⁺ T cells was determined by flow cytometry. Shown is a representative donor (upper panel). Combined data are from three independent donors (n = 3 ± SEM, lower panel). (B,C) CD3⁺ T cells were isolated from mouse splenocytes. T cells were activated using plate-bound anti-CD3 (5 µg/ml) and cultivated in presence of interleukin 2 (IL-2, 100 U/ml) and 0.3 nM of the oligomerized TNF mutants for 4 days. Number of (B) activated CD25⁺TNFR2⁺ T cells and (C) CD25⁺FoxP3⁺ Tregs was determined by flow cytometry. Shown is a representative donor (lower panel). Combined data are from three independent experiments (n = 3 ± SEM, lower panel).

TNFR2 complex formation and signal induction and high bioactivity in *in vitro* and *in vivo* model systems. Our findings, therefore, are of principal relevance for development of TNFR2 agonists for potential therapeutic application. For the use in humans completely human molecules are needed. This can be readily achieved by exchanging the sc-mTNF_{R2} part to its human counterpart scTNF_{R2} which was previously described by our group^{19,21}. The yeast GCN4 tetramerization domain was used here as a model of a coiled-coil structure. To circumvent potential immunogenicity of foreign protein domains, this domain could be exchanged to similar coiled-coil tetramerization domains of human proteins. In addition, other modules and formats resulting in a GCN4-sc-mTNF_{R2}-like configuration are possible to design highly potent TNFR2 agonists.

In summary, our data show that TNFR2 activation by dodecaivalent ligands is clearly superior to trivalent or hexavalent ligands. We also demonstrate that the predicted 3D-structure of a dodecaivalent TNFR2-selective TNF mutant appears to be important for the bioactivity of the ligand. In addition, because of conserved structural features of the members of the TNF/TNFR superfamily, our findings suggest that similar conditions exist for other members of this biologically important cytokine family.

Materials and Methods

Materials. The TNFR2-specific antibody 80M2 has been described¹⁴. The anti-TNF antibody (clone F6C5) was from GeneTex (Irvine, CA) and anti-TNF (HP8001) from Hycult Biotech (Uden, The Netherlands). The anti-CD3 (clone UCHT1 & 17A2) and anti-TNFR2 antibody (AF-426-PB) were from R&D Systems (Wiesbaden-Nordenstadt, Germany). Fluorescence-labeled antibodies against CD3, CD4, CD25, HLA-DR, TNFR2 and FoxP3 were from Miltenyi Biotech (Bergisch-Gladbach, Germany). Secondary antibodies coupled to Alexa Fluor 488 or Alexa Fluor 546 were from Life Technologies (Karlsruhe, Germany) and horseradish peroxidase (HRP)-labeled anti-mouse IgG antibodies were purchased by Jackson ImmunoResearch Laboratories (Suffolk, UK). Recombinant interleukin 2 (IL-2) was purchased by Immunotools (Friesoythe, Germany). Actinomycin D, 4',6-Diamidin-2-phenylindol (DAPI) and 3-(4,5-dimethyl-2-thiazolyl)-2,5-diphenyl-2H-tetrazolium bromide (MTT) were from Sigma-Aldrich and 3,3',5,5'-tetramethylbenzidine (TMB) substrate was purchased from Biogen (San Diego, CA). All other chemicals were of analytical grade.

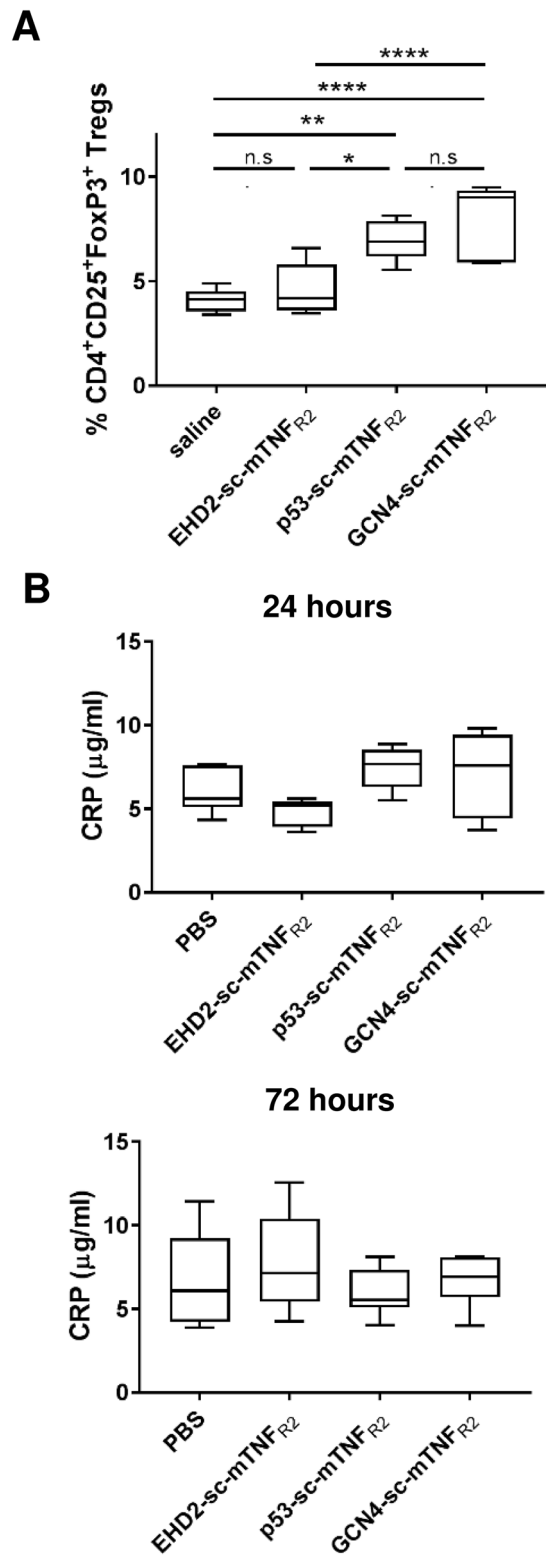


Figure 7. Dodecameric TNF mutants most potently induce T cell activation and Treg expansion C57BL/6 mice were administered with 1 mg/kg body weight (i.p.) of the proteins or saline. **(A)** After 3 days, splenocytes were isolated and number of CD4⁺CD25⁺FoxP3⁺ Tregs was determined by flow cytometry. **(B)** After 24 hours and 72 hours whole blood was withdrawn and CRP levels in the blood were determined by ELISA (n = 5–7 mice ± SEM).

Production and purification of TNFR2 agonists. Production and purification of recombinant proteins was described previously²¹. Briefly, HEK293-6E cells, grown in F17 medium (Life Technologies, Darmstadt, Germany), were transiently transfected with expression constructs of TNF muteins using polyethylenimine (Sigma). The day after, Tryptone N1 (Organotechnie, TekniScience, Terrebonne, Canada) was added to the cell culture and cells were cultivated for additional 4 days. Then, supernatant was collected and recombinant proteins were purified by immobilized metal ion chromatography (IMAC). For this purpose, supernatant was loaded onto a column containing Ni-NTA agarose (Macherey-Nagel, Düren, Germany) and unbound proteins were washed away using IMAC wash buffer (50 mM sodium-phosphate-buffer). Bound proteins were eluted with IMAC elution buffer (50 mM sodium-phosphate-buffer, 250 mM imidazole) and dialyzed (cut-off 4–6 kDa, Roth, Karlsruhe, Germany) against PBS overnight at 4°C. Finally, eluted proteins were purified by SEC. Protein concentration was determined by measuring the absorbance at 280 nm. For coomassie staining, 2 µg of the purified TNF muteins were denatured in Laemmli buffer, resolved by 8% SDS-PAGE and stained with coomassie.

HPLC. Approx. 20 µg protein was applied to a BioSep-SEC-S2000 column (Phenomenex, Aschaffenburg, Germany) equilibrated with PBS and eluted at a flow rate of 0.5 ml/min. For determining the size of recombinant proteins, standard proteins were run under the same conditions.

TNFR binding assay. ELISA plates (Greiner, Frickenhausen, Germany) were coated with TNFR1-Fc or TNFR2-Fc fusion proteins at 1 µg/ml in PBS and incubated at 4°C overnight. Residual binding sites were blocked with 2% skim milk powder in PBS at RT for 2 hours. TNF muteins were diluted in 2% skim milk powder in PBS and incubated for 1 hour at RT. Bound proteins were detected with mouse monoclonal antibodies to TNF (clone F6C5; 1 µg/ml; incubation for 1 hour at RT) and HRP-conjugated anti-mouse IgG antibodies (diluted 1:10000; incubation for 1 hour at RT), followed by incubation with TMB substrate solution. Reaction was stopped by addition of 1 M H₂SO₄ and the absorbance at 450 nm was determined with an absorbance reader (Multiskan FC, Thermo Scientific, Karlsruhe, Germany) and data were analyzed using the software Microsoft Excel and GraphPad Prism 4 (GraphPad, La Jolla, CA). Between each step, non-bound proteins were removed by washing 4 times with 0.005% Tween-20 in PBS.

Attana. Affinities of the oligomerized fusion proteins for TNFR2-Fc were determined by quartz crystal microbalance measurements (Attana Cell 200, Attana, Stockholm, Sweden). Therefore, TNFR2-Fc fusion proteins were chemically immobilized on a carboxyl sensor chip according to the manufacturer's protocol at a high (270 Hz) and low (130 Hz) density, respectively. Binding experiments were performed in PBST (PBS, 0.1% Tween 20) pH 7.4 at a flow rate of 25 ml/min at 37°C. The chip was regenerated with 10 mM Glycine HCl pH 2.0. Before each measurement, a baseline was measured which was subtracted from the binding curve. Data were collected using Attaché Office software (Attana, Stockholm, Sweden) and TraceDrawer (Ridgview Instruments, Vange, Sweden).

Cytotoxicity assay. L929 or Kym-1 cells (1.5×10^4 cells/well) were grown in 96-well flat bottom cell culture plates overnight. L929 cells were treated with actinomycin D (1 µg/ml) and Kym-1 cells with 80M2 (1 µg/ml) for 30 minutes prior to addition of TNF muteins. L929 and Kym-1 cells were incubated with different concentrations of TNF muteins for 24 hours at 37°C. Cells were washed with PBS and incubated with crystal violet (20% methanol; 0.5% crystal violet) for 20 minutes to stain viable cells. The dye was washed away under rinsing water and cells were air-dried. Crystal violet was resolved with methanol and the optical density at 550 nm was determined. Each sample was analyzed in triplicates and data were analyzed using the software Microsoft Excel and GraphPad Prism (GraphPad, La Jolla, CA).

Enzyme-linked immunosorbent assay. BV-2 or HeLa cells were stimulated as indicated, supernatants were collected after 24 hours and analyzed by an ELISA specific for Cxcl-2 (BV-2, R&D Systems, Minneapolis MN) or IL-6 (HeLa, Biolegend, San Diego CA) according to the instructions of the manufacturer. For determination of inflammatory marker CRP in the blood, whole blood was withdrawn and analyzed by an ELISA specific for mouse CRP (R&D Systems, Minneapolis MN) according to the instructions of the manufacturer. The absorbance at 450 nm was determined and the amount of released Cxcl-2 or IL-6 was determined with the provided standard and calculated using the software GraphPad Prism.

Thymocyte proliferation. Thymus of C57BL/6 mice was isolated and mashed through a 40 µm cell strainer (Falcon). Cells were centrifuged (300 g, 5 min) and washed once with culture medium (RPMI 1640, 10% FCS, 50 µM β-mercaptoethanol and penicillin/streptomycin). Then 1.5×10^5 cells were plated into αCD3 coated (6 h at 4°C, 1 µg/ml) 96-well (U) plates and cultivated for 4 days in presence of the oligomerized fusion proteins. Number of cells was determined by MTT (3-(4,5-Dimethylthiazol-2-yl)-2,5-Diphenyltetrazolium Bromide) assay. Therefore, cells were incubated with MTT (0.5 mg/ml) for 2 hours at 37°C. Then lysis buffer (10% SDS, 20 nM HCl) was added, cells were lysed overnight and optical density at 550 nm was determined. Each sample was analyzed in triplicates and data were analyzed using the software Microsoft Excel and GraphPad Prism.

Biological samples. Blood was obtained from volunteer donors, from whom informed consent was obtained. Blood withdrawal was carried out in accordance with relevant guidelines and regulations and all experimental protocols were approved by Ethik-Kommission Universitätsklinikum Tübingen (Project number 283/2014B02).

Human T cell isolation and culture. Blood of volunteer human donors was diluted 1:2 with RPMI medium. Then 30 ml diluted blood was layered over 10 ml Histopaque-1077 (Sigma-Aldrich) and centrifuged for 20 min at 800 g without brake. Interphase, including mononuclear cells of peripheral blood (PBMCs) was

removed and washed with 30 ml RPMI (300 g, 5 min). For removal of platelets, cells were resuspended in 40 ml RPMI and centrifuged for 5 min at 200 g. Then, CD3⁺ T cells were isolated by magnetic separation using the Pan T Cell Isolation Kit (Miltenyi Biotech). Purified T cells were plated in X-Vivo 15 medium (Lonza) in α CD3 coated (6 h at 4 °C) 96-well (U form) plates for T cell activation. Cells were incubated in presence of IL-2 and the oligomerized fusion proteins for 4 days. Then surface expression of CD25 and HLA-DR was determined by flow cytometry according to manufacturer's instructions (Miltenyi Biotech, Bergisch-Gladbach). At least 20,000 cells per sample were acquired. Data were acquired using a MACSQuant Analyzer 10 (Miltenyi) and analyzed with FlowJo (FlowJo, LLC, Ashland, Oregon).

Mouse T cell isolation and culture. Splens from C57BL/6 wildtype mice were dissociated through a 40 μ m cell strainer and collected in 10 ml MACS buffer (PBS, 0.5% BSA, 2 mM EDTA). Splenocytes were centrifuged (300 g, 5 min) and washed once with 10 ml MACS buffer. Then CD3⁺ T cells were isolated using the FACS Aria III and plated in α CD3 coated (6 h at 4 °C) 96-well (U form) plates for T cell activation. T cells were cultivated in presence of IL-2 and the oligomerized fusion proteins for 4 days. Then expression of CD25, TNFR2 and/or FoxP3 was determined by flow cytometry according to manufacturer's instructions (Miltenyi Biotech, Bergisch-Gladbach). Data were acquired using a MACSQuant Analyzer 10 (Miltenyi) and analyzed with FlowJo (FlowJo, LLC).

In vivo Treg assay. Animal care and treatment were carried out in accordance with Committee Stuttgart (Regierungspräsidium Stuttgart) guidelines on the use of experimental animals at the University of Stuttgart. Animal experiments were approved by Regierungspräsidium Stuttgart (permit no. 35-9185.81/0422). Oligomerized fusion proteins (1 mg/kg) were administered intraperitoneal (i.p.) to C57BL/6 wild type mice. After 3 days a second injection (1 mg/kg) was applied. After 7 days, spleens were extracted and splenocytes were isolated. Therefore, spleens were dissociated through a 40 μ m cell strainer and collected in 10 ml MACS buffer (PBS, 0.5% BSA, 2 mM EDTA). Splenocytes were centrifuged (300 g, 5 min) and incubated in 3 ml RBC buffer (0.15 M NH₄Cl, 10 mM KHCO₃, 0.1 M EDTA) per spleen for 5 minutes at room temperature to lyse red blood cells. Then 10 ml MACS buffer was added and splenocytes were centrifuged for 5 min at 300 g. Cells were washed once with 10 ml MACS buffer (5 min, 300 g) and afterwards collected in MACS buffer. Expression of markers CD25 and FoxP3, within the subpopulation of CD4⁺ T cells, was determined by flow cytometry according to manufacturer's instructions (Miltenyi Biotech, Bergisch-Gladbach). Data were acquired using a MACSQuant Analyzer 10 (Miltenyi) and analyzed with FlowJo (FlowJo, LLC).

Quantification of TNF/TNFR2 complex clustering. BV-2 cells were stimulated with TNF muteins for 15 minutes at 37 °C. Then cells were immediately washed two times with ice cold PBS and fixed with 4% PFA in PBS solution. Then unspecific binding sites were blocked with 4% BSA in PBS and cells were incubated with antibodies against TNF (HP8001, Hbt) and TNFR2 (AF-426-PB, R&D systems), followed by detection with appropriate fluorescence labeled antibodies. Nuclei were counterstained with DAPI. Stainings were analyzed on a Zeiss Axio Observer Spinning Disc microscope equipped with a Plan-Apochromat 63x/1.4 Oil DIC objective and an Axiocam 503 mono CCD camera. The following excitation lasers and emission filters were used: DAPI: 405 diode laser, 450/50 nm filter; GFP, 488 nm diode laser, 525/50 nm filter; RFP, 561 nm (RFP) diode laser, 600/50 nm filter. Z-stacks of tile regions containing 6 \times 6 images were acquired and maximum intensity projections were calculated. Image processing was done in Zen blue 2.1 software (Zeiss, Germany).

Quantitative image analysis was done with CellProfiler version 2.2⁵¹. Nuclei were segmented via the DAPI staining and a 120 pixel wide ring mask was drawn around each nucleus representing the cell mask. TNF Vesicles were segmented under the cell mask using the A488 staining and unified for each cell. Mean intensity of the TNFR2 signal using the A546 staining was measured under the unified vesicles representing the grade of co-localized vesicles between TNFR2 (red) and TNF (green) per cell.

Statistics. Data are presented as mean \pm standard error of the mean (SEM) of *n* independent experiments. Normal distribution was analyzed by Shapiro-Wilk normally test. Statistical analyses were performed by Student's t-test or analysis of variance, followed by a post hoc Tukey's range test. **P* < 0.05 (***P* < 0.01; ****P* < 0.001; *****P* < 0.0001) was considered significant.

References

- Bodmer, J. L., Schneider, P. & Tschopp, J. The molecular architecture of the TNF superfamily. *Trends Biochem Sci* **27**, 19–26 (2002).
- Fesik, S. W. Insights into programmed cell death through structural biology. *Cell* **103**, 273–282 (2000).
- Locksley, R. M., Killeen, N. & Lenardo, M. J. The TNF and TNF receptor superfamilies: integrating mammalian biology. *Cell* **104**, 487–501 (2001).
- Berg, D. *et al.* Enforced covalent trimerization increases the activity of the TNF ligand family members TRAIL and CD95L. *Cell Death Differ* **14**, 2021–2034, doi:10.1038/sj.cdd.4402213 (2007).
- Henkler, F. *et al.* The extracellular domains of FasL and Fas are sufficient for the formation of supramolecular FasL-Fas clusters of high stability. *J Cell Biol* **168**, 1087–1098, doi:10.1083/jcb.200501048 (2005).
- Mundle, S. D. & Raza, A. Defining the dynamics of self-assembled Fas-receptor activation. *Trends Immunol* **23**, 187–194 (2002).
- Wyzgol, A. *et al.* Trimer stabilization, oligomerization, and antibody-mediated cell surface immobilization improve the activity of soluble trimers of CD27L, CD40L, 41BBL, and glucocorticoid-induced TNF receptor ligand. *J Immunol* **183**, 1851–1861, doi:10.4049/jimmunol.0802597 (2009).
- Black, R. A. *et al.* A metalloproteinase disintegrin that releases tumour-necrosis factor- α from cells. *Nature* **385**, 729–733, doi:10.1038/385729a0 (1997).
- Smith, R. A. & Baglioni, C. The active form of tumor necrosis factor is a trimer. *J Biol Chem* **262**, 6951–6954 (1987).
- Krippner-Heidenreich, A. *et al.* Single-chain TNF, a TNF derivative with enhanced stability and antitumoral activity. *J Immunol* **180**, 8176–8183 (2008).

11. Fischer, R. & Maier, O. Interrelation of oxidative stress and inflammation in neurodegenerative disease: role of TNF. *Oxid Med Cell Longev* **2015**, 610813, doi:10.1155/2015/610813 (2015).
12. Wajant, H., Pfizenmaier, K. & Scheurich, P. Tumor necrosis factor signaling. *Cell Death Differ* **10**, 45–65, doi:10.1038/sj.cdd.4401189 (2003).
13. Fischer, R., Kontermann, R. & Maier, O. Targeting sTNF/TNFR1 Signaling as a New Therapeutic Strategy. *Antibodies* **4**, 48–70, doi:10.3390/antib4010048 (2015).
14. Grell, M. *et al.* The transmembrane form of tumor necrosis factor is the prime activating ligand of the 80 kDa tumor necrosis factor receptor. *Cell* **83**, 793–802 (1995).
15. Grell, M., Wajant, H., Zimmermann, G. & Scheurich, P. The type 1 receptor (CD120a) is the high-affinity receptor for soluble tumor necrosis factor. *Proc Natl Acad Sci USA* **95**, 570–575 (1998).
16. Krippner-Heidenreich, A. *et al.* Control of receptor-induced signaling complex formation by the kinetics of ligand/receptor interaction. *J Biol Chem* **277**, 44155–44163, doi:10.1074/jbc.M207399200 (2002).
17. Bryde, S. *et al.* Tumor necrosis factor (TNF)-functionalized nanostructured particles for the stimulation of membrane TNF-specific cell responses. *Bioconjug Chem* **16**, 1459–1467, doi:10.1021/bc0501810 (2005).
18. Schneider, P. *et al.* Conversion of membrane-bound Fas(CD95) ligand to its soluble form is associated with downregulation of its proapoptotic activity and loss of liver toxicity. *J Exp Med* **187**, 1205–1213 (1998).
19. Fischer, R. *et al.* A TNF receptor 2 selective agonist rescues human neurons from oxidative stress-induced cell death. *PLoS One* **6**, e27621, doi:10.1371/journal.pone.0027621 (2011).
20. Rauer, H. *et al.* Membrane tumor necrosis factor (TNF) induces p100 processing via TNF receptor-2 (TNFR2). *J Biol Chem* **285**, 7394–7404, doi:10.1074/jbc.M109.037341 (2010).
21. Dong, Y. *et al.* Essential protective role of tumor necrosis factor receptor 2 in neurodegeneration. *Proc Natl Acad Sci USA* **113**, 12304–12309, doi:10.1073/pnas.1605195113 (2016).
22. Seifert, O. *et al.* Tetravalent antibody-scTRAIL fusion proteins with improved properties. *Mol Cancer Ther* **13**, 101–111, doi:10.1158/1535-7163.MCT-13-0396 (2014).
23. Jeffrey, P. D., Gorina, S. & Pavletich, N. P. Crystal structure of the tetramerization domain of the p53 tumor suppressor at 1.7 angstroms. *Science* **267**, 1498–1502 (1995).
24. Pluckthun, A. & Pack, P. New protein engineering approaches to multivalent and bispecific antibody fragments. *Immunotechnology* **3**, 83–105 (1997).
25. Rheinhecker, M. *et al.* Multivalent antibody fragments with high functional affinity for a tumor-associated carbohydrate antigen. *J Immunol* **157**, 2989–2997 (1996).
26. Harbury, P. B., Zhang, T., Kim, P. S. & Alber, T. A switch between two-, three-, and four-stranded coiled coils in GCN4 leucine zipper mutants. *Science* **262**, 1401–1407 (1993).
27. Pack, P., Muller, K., Zahn, R. & Pluckthun, A. Tetravalent miniantibodies with high avidity assembling in Escherichia coli. *J Mol Biol* **246**, 28–34 (1995).
28. Liu, J. *et al.* A parallel coiled-coil tetramer with offset helices. *Biochemistry* **45**, 15224–15231, doi:10.1021/bi061914m (2006).
29. Wallach, D. *et al.* Soluble and cell surface receptors for tumor necrosis factor. *Agents Actions Suppl* **35**, 51–57 (1991).
30. Holler, N. *et al.* Two adjacent trimeric Fas ligands are required for Fas signaling and formation of a death-inducing signaling complex. *Mol Cell Biol* **23**, 1428–1440 (2003).
31. Grell, M., Scheurich, P., Meager, A. & Pfizenmaier, K. TR60 and TR80 tumor necrosis factor (TNF)-receptors can independently mediate cytotoxicity. *Lymphokine Cytokine Res* **12**, 143–148 (1993).
32. Chen, X., Baumel, M., Mannel, D. N., Howard, O. M. & Oppenheim, J. J. Interaction of TNF with TNF receptor type 2 promotes expansion and function of mouse CD4+CD25+ T regulatory cells. *J Immunol* **179**, 154–161 (2007).
33. Chen, X. *et al.* Expression of costimulatory TNFR2 induces resistance of CD4+ FoxP3- conventional T cells to suppression by CD4+ FoxP3+ regulatory T cells. *J Immunol* **185**, 174–182, doi:10.4049/jimmunol.0903548 (2010).
34. Chen, X. *et al.* Cutting edge: expression of TNFR2 defines a maximally suppressive subset of mouse CD4+CD25+ FoxP3+ T regulatory cells: applicability to tumor-infiltrating T regulatory cells. *J Immunol* **180**, 6467–6471 (2008).
35. Chen, X. & Oppenheim, J. J. TNF- α : an activator of CD4+ FoxP3+ TNFR2+ regulatory T cells. *Curr Dir Autoimmun* **11**, 119–134, doi:10.1159/000289201 (2010).
36. Chen, X. *et al.* TNFR2 is critical for the stabilization of the CD4+ Foxp3+ regulatory T cell phenotype in the inflammatory environment. *J Immunol* **190**, 1076–1084, doi:10.4049/jimmunol.1202659 (2013).
37. Okubo, Y., Mera, T., Wang, L. & Faustman, D. L. Homogeneous expansion of human T-regulatory cells via tumor necrosis factor receptor 2. *Sci Rep* **3**, 3153, doi:10.1038/srep03153 (2013).
38. Chopra, M. *et al.* Exogenous TNFR2 activation protects from acute GvHD via host T reg cell expansion. *J Exp Med* **213**, 1881–1900, doi:10.1084/jem.20151563 (2016).
39. Bossen, C. *et al.* TACI, unlike BAFF-R, is solely activated by oligomeric BAFF and APRIL to support survival of activated B cells and plasmablasts. *Blood* **111**, 1004–1012, doi:10.1182/blood-2007-09-110874 (2008).
40. Muller, N., Wyzgol, A., Munkel, S., Pfizenmaier, K. & Wajant, H. Activity of soluble OX40 ligand is enhanced by oligomerization and cell surface immobilization. *FEBS J* **275**, 2296–2304, doi:10.1111/j.1742-4658.2008.06382.x (2008).
41. Wajant, H. *et al.* Differential activation of TRAIL-R1 and -2 by soluble and membrane TRAIL allows selective surface antigen-directed activation of TRAIL-R2 by a soluble TRAIL derivative. *Oncogene* **20**, 4101–4106, doi:10.1038/sj.onc.1204558 (2001).
42. Haswell, L. E., Glennie, M. J. & Al-Shamkhani, A. Analysis of the oligomeric requirement for signaling by CD40 using soluble multimeric forms of its ligand, CD154. *Eur J Immunol* **31**, 3094–3100, doi:10.1002/1521-4141(2001010) (2001).
43. Stone, G. W. *et al.* Multimeric soluble CD40 ligand and GITR ligand as adjuvants for human immunodeficiency virus DNA vaccines. *J Virol* **80**, 1762–1772, doi:10.1128/JVI.80.4.1762-1772.2006 (2006).
44. Aoki, K. *et al.* Extracellular matrix interacts with soluble CD95L: retention and enhancement of cytotoxicity. *Nat Immunol* **2**, 333–337, doi:10.1038/86336 (2001).
45. Hendriks, J. *et al.* Heparan sulfate proteoglycan binding promotes APRIL-induced tumor cell proliferation. *Cell Death Differ* **12**, 637–648, doi:10.1038/sj.cdd.4401647 (2005).
46. Ingold, K. *et al.* Identification of proteoglycans as the APRIL-specific binding partners. *J Exp Med* **201**, 1375–1383, doi:10.1084/jem.20042309 (2005).
47. Ban, L. *et al.* Strategic internal covalent cross-linking of TNF produces a stable TNF trimer with improved TNFR2 signaling. *Mol Cell Ther* **3**, 7, doi:10.1186/s40591-015-0044-4 (2015).
48. Ranzinger, J. *et al.* Nanoscale arrangement of apoptotic ligands reveals a demand for a minimal lateral distance for efficient death receptor activation. *Nano Lett* **9**, 4240–4245, doi:10.1021/nl902429b (2009).
49. Probert, L. TNF and its receptors in the CNS: The essential, the desirable and the deleterious effects. *Neuroscience* **302**, 2–22, doi:10.1016/j.neuroscience.2015.06.038 (2015).
50. Dong, Y., Dekens, D., De Deyn, P., Naudé, P. & Eisel, U. Targeting of Tumor Necrosis Factor Alpha Receptors as a Therapeutic Strategy for Neurodegenerative Disorders. Vol. 4 (2015).
51. Carpenter, A. E. *et al.* CellProfiler: image analysis software for identifying and quantifying cell phenotypes. *Genome Biol* **7**, R100, doi:10.1186/gb-2006-7-10-r100 (2006).

Acknowledgements

This work was supported by a Carl Zeiss Foundation grant (Az. 0563-2.8./508/2) awarded to R.F. We thank Alexandra Kraske and Beatrice Reiser for animal care and Prof. Matthias Schwab and Dr. Svitlana Igel (Dr. Margarete Fischer-Bosch-Institute of Clinical Pharmacology, Robert Bosch Hospital, Stuttgart) for providing human blood. The TNFR2 agonists described in this work can be obtained via a material transfer agreement (MTA).

Author Contributions

R.F., J.M., C.G., S.E. and N.P. conducted experiments. J.M., C.G., S.E., N.P. and J.B. designed parts of the experimental work, analyzed results and contributed to writing the manuscript. R.F., K.P. and R.K. designed and supervised the project, analyzed the results and wrote the manuscript.

Additional Information

Supplementary information accompanies this paper at doi:[10.1038/s41598-017-06993-4](https://doi.org/10.1038/s41598-017-06993-4)

Competing Interests: R.F., K.P. and R.K. are named inventors on patent applications covering the oligomerized TNFR2 agonist technology.

Publisher's note: Springer Nature remains neutral with regard to jurisdictional claims in published maps and institutional affiliations.



Open Access This article is licensed under a Creative Commons Attribution 4.0 International License, which permits use, sharing, adaptation, distribution and reproduction in any medium or format, as long as you give appropriate credit to the original author(s) and the source, provide a link to the Creative Commons license, and indicate if changes were made. The images or other third party material in this article are included in the article's Creative Commons license, unless indicated otherwise in a credit line to the material. If material is not included in the article's Creative Commons license and your intended use is not permitted by statutory regulation or exceeds the permitted use, you will need to obtain permission directly from the copyright holder. To view a copy of this license, visit <http://creativecommons.org/licenses/by/4.0/>.

© The Author(s) 2017